

NMR imaging estimates of muscle volume and intramuscular fat infiltration in the thigh: variations with muscle, gender, and age

Jean-Yves Hogrel · Yoann Barnouin · Noura Azzabou · Gillian Butler-Browne · Thomas Voit · Amélie Moraux · Gaëlle Leroux · Anthony Behin · Jamie S. McPhee · Pierre G. Carlier

Received: 14 April 2015 / Accepted: 25 May 2015 / Published online: 4 June 2015
© American Aging Association 2015

Abstract Muscle mass is particularly relevant to follow during aging, owing to its link with physical performance and autonomy. The objectives of this work were to assess muscle volume (MV) and intramuscular fat (IMF) for all the muscles of the thigh in a large population of young and elderly healthy individuals using magnetic resonance imaging (MRI) to test the effect of gender and age on MV and IMF and to determine the best representative slice for the estimation of MV and IMF. The study enrolled 105 healthy young (range 20–30 years) and older (range

70–80 years) subjects. MRI scans were acquired along the femur length using a three-dimension three-point Dixon proton density-weighted gradient echo sequence. MV and IMF were estimated from all the slices. The effects of age and gender on MV and IMF were assessed. Predictive equations for MV and IMF were established using a single slice at various femur levels for each muscle in order to reduce the analysis process. MV was decreased with aging in both genders, particularly in the quadriceps femoris. IMF was largely increased with aging in men and, to a lesser extent, in women. Percentages of MV decrease and IMF increase with aging varied according to the muscle. Predictive equations to predict MV and IMF from single slices are provided and were validated. This study is the first one to provide muscle volume and intramuscular fat infiltration in all the muscles of the thigh in a large population of young and elderly healthy subjects.

Electronic supplementary material The online version of this article (doi:10.1007/s11357-015-9798-5) contains supplementary material, which is available to authorized users.

J.-Y. Hogrel (✉) · Y. Barnouin · N. Azzabou · G. Butler-Browne · T. Voit · A. Moraux · G. Leroux · P. G. Carlier
UPMC UM 76, INSERM U 974, CNRS UMR 7215, Institut de Myologie, GH Pitié-Salpêtrière, Paris, France
e-mail: jy.hogrel@institut-myologie.org

A. Behin
AP-HP, Centre de Référence de Pathologies Neuromusculaire Paris Est, Institut de Myologie, GH Pitié-Salpêtrière, Paris, France

J. S. McPhee
School of Healthcare Science, Manchester Metropolitan University, Manchester, UK

N. Azzabou · P. G. Carlier
CEA, I2BM, MIRCen, IdM NMR Laboratory, Institut de Myologie, GH Pitié-Salpêtrière, Paris, France

Keywords Muscle volume · Intramuscular fat · Magnetic resonance imaging · Anatomical cross-sectional area · Thigh muscles

Introduction

Quantifying muscle mass is particularly relevant not only to assess and manage muscle atrophy during aging (Narici et al. 2003; Morse et al. 2005a) but also to

determine the impact of muscle quantity changes on muscle performance. Nuclear magnetic resonance (NMR) imaging is acknowledged as one of the best methods to assess muscle volume (MV). MV is generally computed from several contiguous muscle anatomical cross-sectional areas (ACSAs), depending on the measurement precision required. An estimate of strength efficiency may also be computed as maximal strength divided by muscle ACSA and is often used as an indicator of muscle quality (Delmonico et al. 2009).

In order to reduce the time and the cost of image processing, the authors have proposed to estimate MV from a single slice. Indeed, complete segmentation of all the muscles of an entire thigh may take between 3 and 4 h. Morse et al. (2007) showed that only one quadriceps femoris muscle (QUAD) ACSA taken at 60 % of the femur length (distal to proximal) could estimate QUAD volume with a standard error of estimate of 9.9 ± 5.7 %. These authors used a third-order polynomial regression model to estimate the ACSA at 60 % that was only validated in young men and confined to the QUAD. Cotofana et al. (2010) showed that the best correlation coefficients between ACSA and MV calculated at different femur levels varied according to the muscle studied. Best correlations were found at 20–40 % (proximal to distal level) for the extensor muscles, 70 % for the flexor muscles, 30 % for the adductor muscles, and 70 % for the sartorius muscle. These authors mentioned that the best correlation was found nearly at the maximal ACSA of each muscle, keeping in mind that the different thigh muscles do not have their maximal ACSA at mid-length. In both of these studies, the population tested was very restricted (18 young men and 41 perimenopausal women respectively) and probably not representative of the whole healthy population. Moreover, only results on muscle groups and not on individual muscles were provided.

Previous reports have observed an accumulation of fat within muscles during aging (Forsberg et al. 1991; Frantzell and Ingelmark 1951; Hasson et al. 2011), which also results in a loss of functional muscle mass. Using MRI, Kent-Braun et al. (2000) have reported a similar trend of intramuscular fat (IMF) accumulation in the ankle dorsiflexor muscles with age in both genders. Hasson et al. (2011) have recently shown that IMF within the dorsi- and plantar-flexor muscles was muscle-dependent and distributed nonlinearly along the leg. These authors described that absolute amounts of adipose tissue infiltration within the muscle were

constant along the muscle length with consequently the lowest proportion near the maximal ACSA.

Emerging evidence suggests that IMF accumulation is associated with muscle atrophy, increased risk of physical limitation, or poor habitual physical activity level (Visser et al. 2002; Hasson et al. 2011; Leskinen et al. 2009) and that it is relevant to investigate lipid metabolism in skeletal muscle (Stein and Wade 2005). This is why estimating IMF accumulation recently gained attention. Although the impact and mechanism of IMF in sarcopenia or dynapenia are still unclear, it follows that IMF infiltration in the muscle has direct consequences in the estimation of muscle quantity and muscle quality.

The objectives of this study were (1) to assess MV and IMF for all the muscles of the thigh in a large population of healthy individuals, (2) to test the effect of gender and age on MV and IMF estimates, (3) to determine the best representative slice for the estimation of MV and IMF for the individual muscles of the thigh, the corresponding muscle groups and the whole thigh, and (4) to establish and validate prediction equations to estimate MV and IMF from this single slice.

Methods

Participants

One hundred five healthy French volunteers (35 young subjects aged between 20 and 30 and 70 older subjects aged between 70 and 80) participated in this study as subjects for the MyoAge project (McPhee et al. 2013). Eligible participants were free from contraindications for MRI; neurologic, cardiovascular, or muscle disease; and medications that may affect the study variables. Subjects signed a written informed consent after confirmed eligibility. This research was approved by the local ethics committee (CPP Paris-Ile de France VI-IB number: 2010-A006114-35). Five subjects did not accept to undergo the full MRI protocol due to the length of the exam or claustrophobic feeling. One hundred subjects were thus analyzed. This population was then split into two groups: 72 subjects were used to establish predictive equations for MV and 71 for IMF (one subject was discarded due to the presence of artefacts during the reconstruction process). Twenty-eight subjects aged between 70 and 80 were used as supplementary subjects to

test the validity to estimate MV and IMF from a single slice.

Image acquisition

Bilateral MRI scans of the thighs (from iliac crests to the articular surface of the tibia) were acquired on each subject placed supine in a 3.0 Tesla MRI scanner (Tim Trio, Siemens Healthcare, Erlangen, Germany). In order to avoid movements and minimize compression of the legs, their heels were fixed on a non-metallic support. Muscle ACSA were measured on 5-mm-thick contiguous axial out-of-phase images using a three-dimension three-point Dixon gradient echo sequence (Glover and Schneider 1991) (TE= 2.75/3.95/5.15 ms, one excitation, $448 \times 224 \times 64$ matrix, $448 \times 224 \times 320$ mm³ field of view) to differentiate lean and fat mass. A 3° flip angle and a 10-ms repetition time were used to obtain a proton density weighting. All sequences were performed with a quadrature bird cage body coil for transmission and sets of phased-array receiver coils surrounded the thigh, with 3×6 flexible coils covering the segment and 3×6 coils embedded in the patient table. Neither acceleration nor parallel imaging techniques were used. Image analysis software (Radionet v.2.2.10., Scito, Paris, France) was used for manual segmentation of the thigh muscles. Image acquisition lasted around 6 min for the Dixon sequence.

Dixon techniques rely on the water/fat chemical shift difference and consequently on their phase difference in the NMR signal to separate them with post-processing. The three-point Dixon technique acquires three images with three selected echo time such that the fat and water are, respectively, in phase, opposed phase, and in phase (it can be also opposed phase, in phase, and opposed phase). Contrarily to the two-point Dixon and the extended two-point Dixon methods, the three-point Dixon method brings in better robustness since it deals with B0 inhomogeneities that are assumed to be directly proportional to the phase difference of images acquired at the first and third echo times. Once B0 inhomogeneities are calculated, fat and water signals are obtained through simple linear system solving. It is important to point out that an accurate estimate of B0 inhomogeneities is fundamental for correct fat and water separation and to prevent fat and water swaps. This can be achieved through phase unwrapping techniques such as the one

presented by Abdul-Rahman et al. (2007) that was considered in this work to unwrap the phase difference between the first and third echo time.

MRI measurements

Depending on the stature of the subjects, about 98 MRI slices (± 7 slices) were analyzed to assess all the individual thigh muscles, which, in turn, takes generally 3 to 4 h. Muscles were manually segmented as presented in Fig. 1. Muscle volume was computed using the cylinder method as given by:

$$MV = \sum_{i=1}^{n-1} h \frac{(ACSA_i + ACSA_{(i+1)})}{2}$$

where n is the number of slices used and h is the inter-slice distance.

To avoid the influence of subject height as a possible confounding variable, MV was normalized by the femur length. MV_n is noted in the following and expressed in cm².

The muscles selected for segmentation were the four heads of the QUAD (rectus femoris (RF), vastus lateralis (VL), vastus intermedius (VI), and vastus medialis (VM)), the four muscles composing the hamstrings muscles (HAMST) (biceps femoris short head (BFB), biceps femoris long head (BFL), semitendinosus (ST) and semimembranosus (SM)), adductors (ADDUC: adductor longus, brevis, magnus and pectineus together (AD), and gracilis (GR)), and the sartorius (SA). Because delineations between adductors muscles were not so obvious at proximal part, all adductors muscles were segmented together, except for the GR which was easily recognizable (Fig. 1). Consequently, by summing all the muscle ACSAs at a precise level along the femur length, an estimate of the whole thigh ACSA was also obtained. Visible fat at the muscle periphery, aponeurosis, blood vessels, nerves, and femur bone were excluded as much as possible.

The muscle ACSAs selected for correlation analyses were chosen at 20, 30, 40, 50, 60, 70, and 80 % of femur length (the distal point was taken as 0 %). Femur length was measured as the distance between the bottom of the lateral condyle of the femur and the top of the greater trochanter. Considering these landmarks, some muscles may thus terminate proximally at more than 100 %.

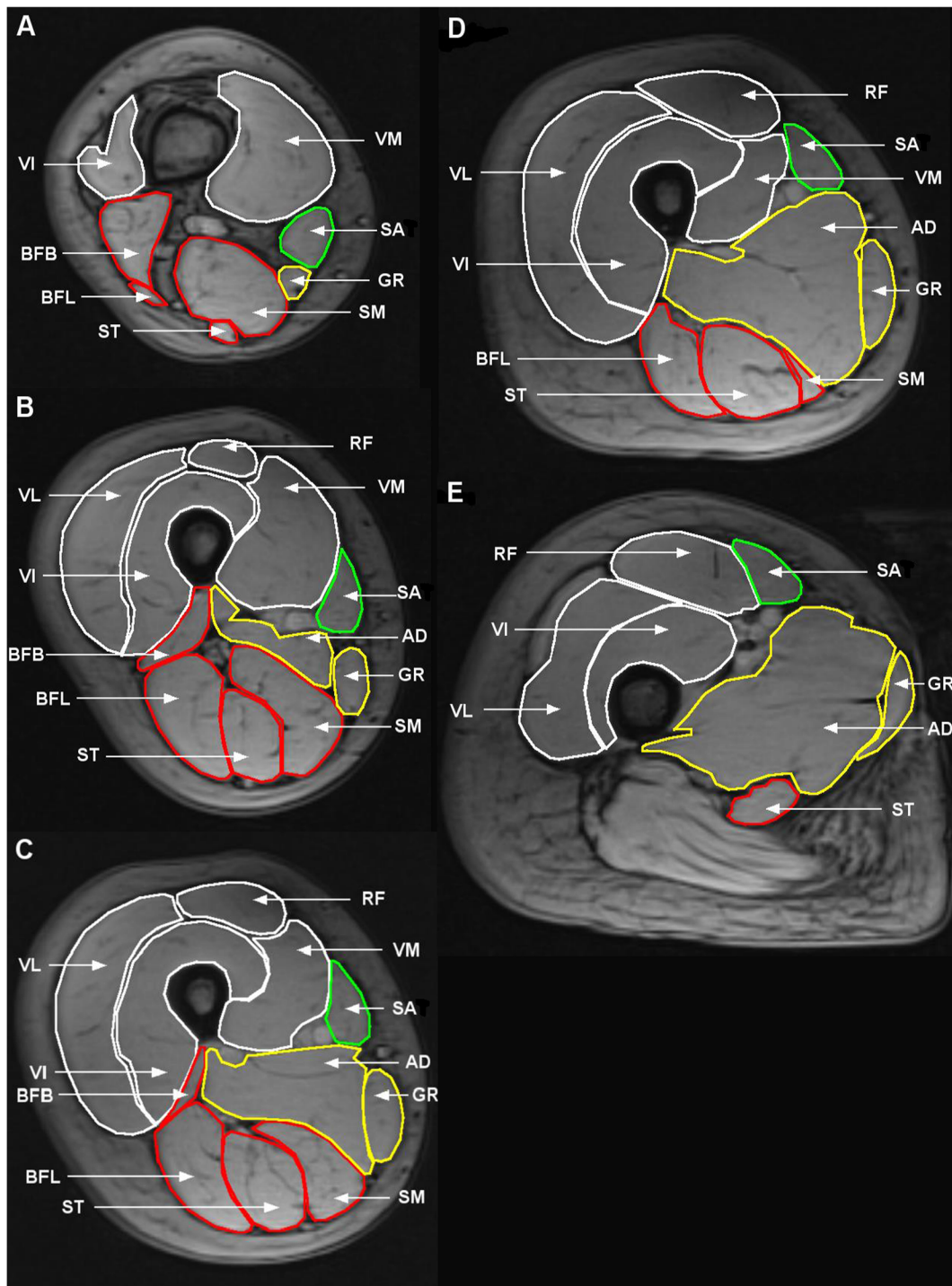


Fig. 1 Illustration of segmented MRI ACSAs of the thigh at **a** 20 %, **b** 40 %, **c** 50 %, **d** 60 %, and **e** 80 % femur length (from distal to proximal). Group muscles are color-coded: QUAD =

white; HAMST = *red*; ADDUC = *yellow*; SA = *green*. Note the exclusion of non-muscular elements (blood vessels, nerves) in the manual segmentation

IMF was computed as already described (Glover and Schneider 1991) in all the individual muscles using the

same inter-slice distance as for MV. Its estimate represents the fraction of NMR signal that is attributable to fat.

Statistical analyses

Statistical analyses were performed using SPSS (version 19.0). The effects of gender and age on MV and IMF and interaction between both factors were assessed using a two-factor ANOVA. Spearman rho was computed to test the relationship between MV and IMF and between BMI and IMF. Linear regressions between ACSA and MV and between IMF computed on all the slices and a single slice were carried out to determine their degree of association and, therefore, the best level to estimate MV and IMF from a single slice, respectively. Estimated MV and IMF were obtained by using linear regression equations. This was done for each muscle, each muscle group, and the whole thigh. Number of subjects, adjusted R^2 , and standard error of estimate (SEE) were used to refine the choice of the slice level. A population of 28 supplementary subjects aged between 70 and 80 was used to validate the prediction equations for the quadriceps femoris muscles for both MV and IMF. SEE was used to quantify the fitting error in the supplementary subjects. The level of statistical significance was set to 0.05.

Results

Participant characteristics

Participant characteristics stratified by sex and age groups are given in Table 1 ($n=72$). Women presented with significantly smaller height, weight, and BMI than men (all $P<0.001$). Older subjects exhibited smaller height and higher BMI than their younger counterparts (all $P<0.001$). However, their weight was not

significantly different. BMI was much more increased in men than in women with aging (interaction between age and gender, $P=0.005$).

Effect of age and gender on muscle volume and intramuscular fat

Figure 2 illustrates a typical example of the effect of aging on thigh muscles where it can be clearly seen in both the atrophic process and the intramuscular fat infiltration. Results showed that all the thigh muscles taken individually were significantly smaller in older subjects compared to the youngest in both genders (all $P<0.001$) (Table 2). Men also exhibited significantly higher MV than women for all the muscles. Statistical analyses also indicated significantly higher IMF percentages (between nearly 1.5 to 2.5-fold increase) in each thigh muscle in older subjects compared to the youngest for both genders (all $P<0.001$) (Table 3). IMF was significantly correlated with BMI for all individual muscles or muscles groups (rho ranging between 0.324 and 0.567; all $P<0.01$). Although relative changes in fat infiltration were generally higher in men, there was not significant age–gender interaction.

Individual muscles and muscle groups presented various percentages of atrophy and intramuscular fat. Comparing older and young subjects, the most atrophied muscles were the muscles of the quadriceps femoris, VM apart (between -37 and -25 % in both genders), and the gracilis muscle (-31 % for men and -25 % for women). Concerning the hamstrings, ST was the most atrophied in men (-28 %), while SM was the most atrophied in women (-24 %).

Table 1 Characteristics of the control population

	Men		Women		Effect (p value)		
	Young $n=18$	Old $n=19$	Young $n=16$	Old $n=19$	Age	Gender	Age \times gender
Age (years)	23.6 (2.9)	74.0 (3.1)	23.9 (2.8)	74.6 (3.3)	<0.001	0.478	0.840
Height (m)	1.79 (0.05)	1.69 (0.07)	1.64 (0.07)	1.58 (0.05)	<0.001	<0.001	0.120
Weight (kg)	71.3 (7.9)	76.0 (10.1)	57.4 (7.1)	56.3 (6.2)	0.331	<0.001	0.128
BMI (kg/m ²)	22.2 (2.2)	26.6 (2.2)	21.4 (2.4)	22.6 (2.4)	<0.001	<0.001	0.005

All values are expressed as mean (standard deviation)

BMI body mass index

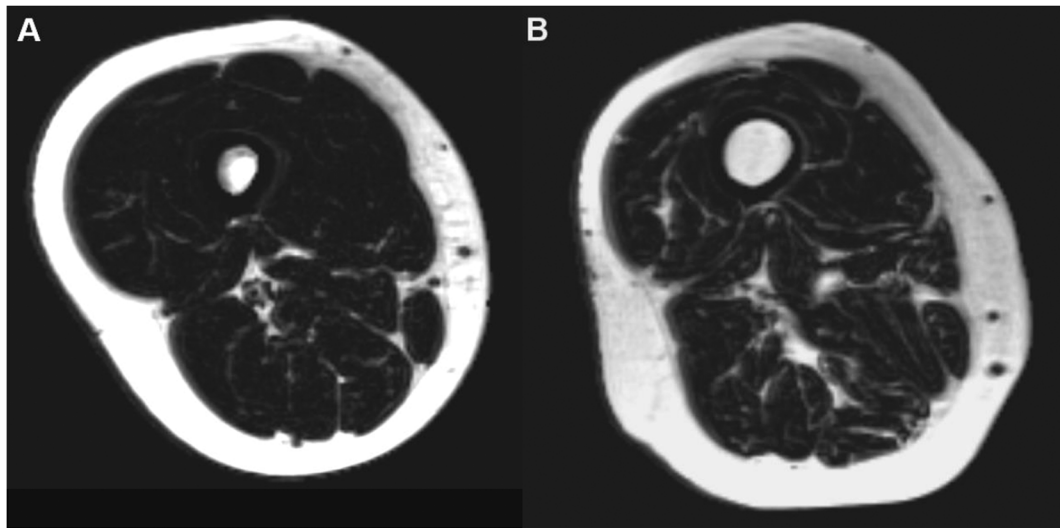


Fig. 2 Comparison of typical axial MRI slices obtained from a young active woman (**a** aged 28 years) and an older active woman (**b** aged 80 years) at 40 % femur length. Note that accumulation of intramuscular fat worsens significantly with aging (along with extramuscular fat)

In young subjects, the most fat-infiltrated muscles were the BFB, GR, and SA in both genders. The largest relative changes were observed for VI, ST, and SM in men and for BFL and ST in women. The BFB was the most preserved muscle

with respect to both muscle volume and fat infiltration with aging.

For each individual muscle or muscle group, a significant correlation between MV_n and IMF was found (Table 4).

Table 2 Effect of age and gender on muscle volume of the individual muscles of the thigh

MV (cm ³)	Men			Women			Effect (<i>p</i> value)		
	Young <i>n</i> =18	Old <i>n</i> =19	% Diff	Young <i>n</i> =16	Old <i>n</i> =19	% Diff	Age	Gender	Age × gender
QUAD	2112.2 (309.5)	1558.4 (287.6)	-26	1294.4 (150.1)	949.2 (101.5)	-27	<0.001	<0.001	0.061
RF	325.0 (59.9)	210.3 (35.6)	-35	196.4 (26.7)	123.0 (19.6)	-37	<0.001	<0.001	0.027
VI	579.2 (78.6)	434.7 (100.7)	-25	356.5 (56.5)	267.7 (38.5)	-25	<0.001	<0.001	0.111
VL	706.5 (117.7)	505.4 (85.7)	-28	437.6 (48.2)	311.7 (36.5)	-29	<0.001	<0.001	0.049
VM	501.5 (79.4)	407.9 (88.8)	-19	303.9 (44.3)	246.8 (30.1)	-19	<0.001	<0.001	0.245
HAMST	827.7 (161.7)	674.3 (99.8)	-19	525.7 (49.1)	439.1 (55.0)	-16	<0.001	<0.001	0.173
BFB	121.3 (30.5)	102.5 (22.2)	-15	69.2 (10.9)	63.9 (10.1)	-8	0.015	<0.001	0.167
BFL	216.1 (45.9)	188.3 (24.1)	-13	144.9 (16.3)	122.6 (17.1)	-15	<0.001	<0.001	0.688
ST	224.2 (52.3)	162.4 (24.8)	-28	131.6 (26.2)	116.0 (29.2)	-12	<0.001	<0.001	0.007
SM	266.1 (61.1)	221.1 (48.2)	-17	179.9 (26.5)	136.6 (29.3)	-24	<0.001	<0.001	0.939
ADDUC	1168.5 (177.1)	977.8 (153.4)	-16	697.2 (96.6)	610.8 (72.3)	-12	<0.001	<0.001	0.100
AD	1031.0 (157.8)	883.0 (145.4)	-14	621.7 (82.6)	554.1 (67.5)	-11	<0.001	<0.001	0.163
GR	137.5 (32.1)	94.8 (18.9)	-31	75.6 (20.6)	56.8 (13.3)	-25	<0.001	<0.001	0.026
SA	180.9 (31.2)	148.5 (21.1)	-18	113.2 (24.0)	91.0 (16.9)	-20	<0.001	<0.001	0.366
THIGH	4290.1 (628.5)	3359.0 (515.7)	-22	2630.5 (278.3)	2090.1 (209.5)	-21	<0.001	<0.001	0.067

All values are expressed as mean (standard deviation)

Table 3 Effect of age and gender on intramuscular fat of the individual muscles of the thigh

IMF (%)	Men			Women			Effect (<i>p</i> value)		
	Young <i>n</i> =18	Old <i>n</i> =19	% Diff	Young <i>n</i> =16	Old <i>n</i> =18	% Diff	Age	Gender	Age× gender
QUAD	2.6 (0.3)	4.7 (1.0)	+81	2.8 (0.5)	4.5 (0.9)	+61	<0.001	0.770	0.284
RF	2.5 (0.3)	4.3 (1.0)	+72	2.8 (0.6)	4.1 (1.0)	+46	<0.001	0.823	0.124
VI	2.4 (0.3)	4.6 (1.4)	+92	2.6 (0.5)	4.3 (1.0)	+65	<0.001	0.410	0.376
VL	3.0 (0.4)	5.4 (1.1)	+80	3.2 (0.5)	5.3 (1.0)	+66	<0.001	0.901	0.765
VM	2.4 (0.3)	4.2 (1.0)	+75	2.6 (0.6)	3.8 (0.8)	+46	<0.001	0.601	0.063
HAMST	3.7 (0.6)	7.5 (1.6)	+103	4.2 (0.8)	8.2 (3.4)	+95	<0.001	0.205	0.818
BFB	4.6 (0.8)	7.6 (1.5)	+65	5.8 (1.3)	7.7 (1.6)	+33	<0.001	0.200	0.383
BFL	3.9 (0.6)	7.2 (1.6)	+85	4.3 (0.6)	8.6 (4.5)	+100	<0.001	0.161	0.389
ST	2.9 (0.5)	6.6 (1.5)	+128	3.7 (0.8)	6.8 (2.2)	+84	<0.001	0.169	0.327
SM	3.7 (0.8)	8.4 (2.3)	+127	4.0 (0.8)	9.9 (7.0)	+47	<0.001	0.329	0.504
ADDUC	3.0 (0.5)	5.3 (1.3)	+77	3.4 (0.5)	5.5 (1.5)	+62	<0.001	0.238	0.543
AD	2.7 (0.4)	5.1 (1.3)	+89	3.1 (0.4)	5.2 (1.5)	+68	<0.001	0.407	0.644
GR	4.6 (0.9)	7.4 (1.6)	+61	6.2 (1.0)	8.4 (1.9)	+35	<0.001	<0.001	0.383
SA	4.6 (0.8)	7.4 (1.5)	+61	5.8 (1.2)	8.3 (1.7)	+68	<0.001	<0.001	0.677
THIGH	3.0 (0.4)	5.6 (1.1)	+87	3.4 (0.5)	5.7 (1.6)	+68	<0.001	0.307	0.713

All values are expressed as mean (standard deviation)

Muscle volume and intramuscular fat estimates from a single slice

A typical example of ACSA profiles for each muscle and each muscle group is illustrated in Fig. 3. An estimate of MV and IMF was computed in ACSA of the thigh at 20, 30, 40, 50, 60, 70, and 80 % of femur length. The correlations between MV (respectively IMF) estimated on all the slices and MV (respectively IMF) estimated from a single slice were dependent on the femur level (Supplementary Tables 1 and 2). The best linear fit was not always found at the same femur level for both MV and IMF, depending on the muscle. Taking into account all of the linear fitting data (merging data from Supplementary Tables 1 and 2), the best estimate of both MV and IMF from a single slice occurred at 50 % for the muscles of the QUAD, 40 % for the muscles of the HAMST, and 60 % for the muscles of the ADDUC. At these thigh levels, Table 5 provides the prediction equations for MV_n (in cm²) and IMF (in %) for each muscle, each muscle group and the entire thigh.

Validation of predictive equations on supplementary subjects

The prediction equations for MV_n and IMF were applied to a group of 28 supplementary subjects for RF, VI, VL,

VM, and QUAD. SEE was close to the SEE values observed for the control population both for MV (RF: 0.59, VI: 0.68, VL: 0.62, VM: 0.86, QUAD: 1.26) and IMF (RF: 0.73, VI: 0.44, VL: 0.52, VM: 0.30, QUAD: 0.30) (see Supplementary Tables 1 and 2). This result proves that the prediction equations for MV and IMF

Table 4 Correlation between MV_n and IMF for each muscle, muscle group, and whole thigh

Muscle	Spearman rho	<i>p</i>
QUAD	-0.449	<0.001
RF	-0.552	<0.001
VI	-0.398	<0.001
VL	-0.506	<0.001
VM	-0.281	0.018
HAMST	-0.328	0.006
BFB	-0.305	0.010
BFL	-0.284	0.017
ST	-0.392	0.005
SM	-0.338	<0.001
ADDUC	-0.362	0.002
AD	-0.313	0.008
GR	-0.655	<0.001
SA	-0.463	<0.001
THIGH	-0.415	<0.001

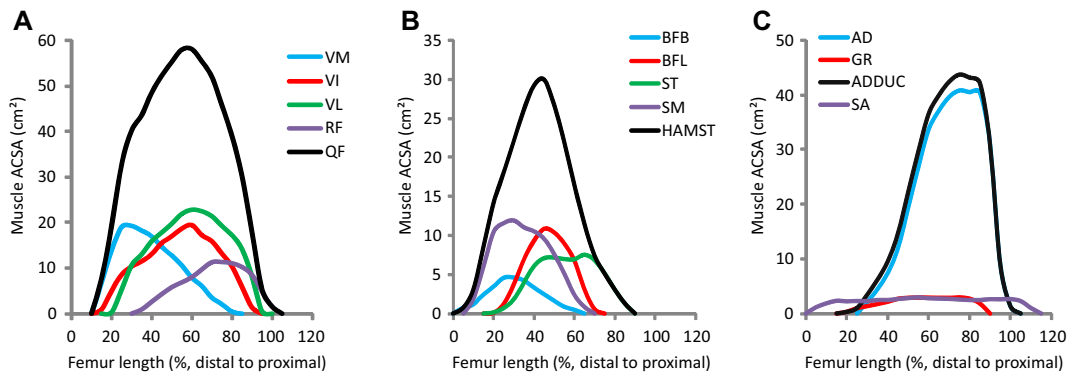


Fig. 3 ACSA profiles. **a** Evolution of the anatomical cross-sectional areas (ACSAs) of the quadriceps muscles and of the whole quadriceps at levels of percentage of the femur length (from distal to proximal). **b** Evolution of the ACSAs of the hamstrings

muscles and of the whole hamstrings at levels of percentage of the femur length. **c** Evolution of the ACSAs of the adductors muscles and sartorius at levels of percentage of the femur length

were also robust for another population than the control population.

Discussion

The present study is the first to provide a complete analysis of individual muscles of the thigh in terms of muscle volume and intramuscular fat infiltration in young and elderly healthy subjects. This paper gives reference values for each individual muscle of the thigh and consequently to the muscle groups and the whole

thigh. It also provides prediction equations to estimate MV and IMF from a single MRI slice.

Our results suggest that age-related loss of thigh muscle mass and increase in intramuscular fat is muscle-dependent, probably due to the fiber-type difference or the type of physical activity which may more or less involve the different thigh muscles depending on the action performed. However, one must keep in mind that our study was cross-sectional. As in previous studies (Macaluso et al. 2002; Maden-Wilkinson et al. 2013; Ogawa et al. 2012), we found that the proportion of QUAD muscle in the total thigh was reduced with aging

Table 5 Prediction equations for MV and IMF from the optimal slice. Muscle volume can be deduced by the following equation: $MV (cm^3) = femur\ length \times (intercept + ACSA (cm^2) \times slope)$. Intramuscular fat within the whole muscle can be computed as: $IMF (\%) = intercept + IMF (\% \text{ within the slice}) \times slope$

Muscles	Muscle volume			Intramuscular fat		
	Intercept	Slope	R ²	Intercept	Slope	R ²
QUAD	1.723	0.567	0.974	0.171	1.060	0.950
RF	0.749	0.717	0.905	0.245	0.993	0.760
VI	0.669	0.481	0.935	0.472	1.047	0.940
VL	0.581	0.529	0.952	0.199	1.020	0.872
VM	1.329	0.556	0.901	0.566	.0931	0.895
HAMST	0.164	0.439	0.922	1.106	0.923	0.981
BFB	0.091	0.522	0.855	2.075	0.914	0.898
BFL	0.211	0.326	0.815	0.908	0.965	0.979
SM	0.613	0.397	0.828	1.051	0.870	0.989
ST	0.687	0.431	0.851	1.090	0.956	0.867
ADDUC	1.851	0.429	0.927	0.165	1.042	0.929
AD	2.084	0.412	0.917	0.060	1.019	0.919
GR	0.133	0.491	0.936	0.165	1.105	0.892
SA	0.258	0.880	0.930	1.679	0.676	0.895
THIGH	1.320	0.607	0.970	0.459	0.972	0.979

because QUAD is more susceptible to muscle atrophy with aging than the other muscle groups. Trappe et al. (2001) suggested that individual muscles of the quadriceps were similarly affected by aging; however, our data support another report that shows the RF was most affected by aging (Maden-Wilkinson et al. 2013), while the VM was better preserved. Atrophy of the QUAD was substantial both in men and women (26 and 27 %, respectively). Data on other muscles are very scarce and this study provides first data on all the individual muscles of the thigh.

Nilwik et al. (2013) found a similar QUAD ACSA as in the present study, but a smaller difference (14 %) between young and old subjects. These differences may be explained by differences in muscle segmentation since we excluded inter-muscular fat in the segmentation process. ACSAs for QUAD and for entire thigh estimated at 50 % were similar to the ACSA at mid-thigh observed in previous studies (Ogawa et al. 2012; Maden-Wilkinson et al. 2013). Atrophy of quadriceps femoris with aging is mainly attributed to reduction in type II muscle fiber size (Nilwik et al. 2013), probably linked to a lack of repairing ability due to a reduced satellite cell content in type II fibers (Verdijk et al. 2007).

Kent-Braun et al. (2000) have selected a single slice corresponding to the largest ACSA using MRI to estimate the percentage of non-contractile area of the ankle dorsiflexor muscles. Non-contractile area, which can be assumed to be mainly fat, was observed to be increased by 132 % in men and 160 % in women with aging. In the muscles of the thigh, intramuscular fat infiltration was found to be highly significant with aging, but variable depending on the muscle. We found similar IMF differences for QUAD (+72 %) and HAMST (+116 %) between young and older men as the ones reported by Overend et al. (1992). Interestingly, IMF was correlated to BMI. Thus, a significant amount of BMI may be explained by IMF, which suggests that IMF plays a non-negligible role in BMI increase in men.

To our knowledge, this is the first study which tests if intramuscular fat estimated from a single MRI slice is representative of fat infiltration computed over entire muscles or muscle groups. Depending on the muscles or muscle groups studied, the distal-to-proximal level of the slice to be analyzed varied. The optimal slice for each muscle was roughly situated where it was the largest, as already observed (Morse et al. 2007; Cotofana et al. 2010). For the entire thigh, the best

estimate for MV and IMF was obtained at 50 % femur length. Therefore, the best way to estimate muscle volume atrophy and intramuscular fat infiltration of the thigh with a single MRI slice consists in segmenting all thigh muscles at the mid-femur level slice which takes less than 10 min. Femur length has also to be estimated since predictive equations for MV used this variable as a normalization factor.

It is important to note here that the three-point Dixon presents several limitations. First, the echo times that were used are not optimal as explained in (Reeder et al. 2005). In order to optimize SNR within the images, the authors recommended a set of asymmetric echo times as well as an iterative algorithm called IDEAL to compute fat and water signals. In spite of his good performances in terms of SNR, this algorithm assumes very low B0 inhomogeneities and converges to local minimum when this condition is not verified which resulted also in a bad fat and water separation. Many solutions were proposed to tackle this problem (Hernando et al. 2008; Hernando et al. 2010; Sharma et al. 2012), but all of them work only for 2D images with a high computation time and they are not available on clinical machines. Furthermore, in the case of our application, the fat content is very low compared to the water one which means that the impact of the selection of echo time on the SNR is minor as shown in (Reeder et al. 2005).

The second limitation of the standard three-point Dixon approach is the oversimplified fat modeling that ignores the actual spectrum of lipids. In fact, this technique underestimates the fat signal because it accounts only for the methylene component in the triglyceride molecules that account for most of body fat. In the studies that introduced more accurate fat spectral models (Hines et al. 2009; Reeder et al. 2009), the authors showed linear relationship between multi- and single peaks fat models using in vivo data and phantoms. Using simulations, it was also shown that a linear relation exists between actual fat signal and the estimated one using three-point Dixon technique (Azzabou et al. 2015). From these studies, one sees that standard Dixon techniques provide fat values that are directly proportional to the actual amounts of fat.

The present study presents other limitations. First, the subjects were all healthy, active, and socially involved and the older group were therefore a homogeneous group of robust, older individuals. Muscle volume, intramuscular fat, and other variables may be much more altered when considering diseased or truly sedentary

older people. Our data are therefore indicative of healthy aging. Second, the results of this study rely on the hypothesis that thigh muscles are homogeneous in terms of fat infiltration, which may not be the case in some disorders (for instance in type 2 diabetes (Karampinos et al. 2012)). Third, the design of the study was cross-sectional which limits the power of the conclusions that can be inferred due to the possible social and secular factors that might influence the direct comparison of older and young subjects. Finally, there are subtle inter-individual variations in muscle shape that may lead to an over- or under-estimate of muscle volume from a single slice measurement.

In conclusion, the present study provides novel quantitative data for all individual thigh muscles in terms of muscle volume and fat infiltration using MRI. The results suggest that a single MRI slice can be representative of a whole muscle, muscle group, or thigh to estimate muscle volume and intramuscular fat infiltration. This provides a simple and practical way to assess muscle quantity and quality, which can also have applications in diseases such as cancer (Argiles et al. 2006), HIV infection (Roubenoff 2000), chronic heart failure (Piepoli et al. 2006) or chronic obstructive pulmonary disease (Vermeeren et al. 2006), bed rest (Kawakami et al. 2000; Kouzaki et al. 2007), or training (Morse et al. 2005b; D'Antona et al. 2006). Finally, because IMF is increased with aging, we suggest considering intramuscular fat infiltration when estimating muscle volume to assess sarcopenia; otherwise, this may underestimate the loss of muscle mass with aging. More work is also needed to determine the reasons why aging leads to a shift in metabolic processes to increase the deposition of fat in muscle and why some muscles are more affected than others.

Acknowledgments This study was funded in part by the EU within the frame of the FP7 Project Myoage (contract n 223576) and the *Association Française contre les Myopathies*. The authors wish to thank the *Comité Départemental de la Retraite Sportive de Paris*, the *Lions Club de Paris*, and their members who volunteered to take part in this study. The authors wish to thank Jean-Marc Boisserie and Julien Le Louër for their skillful assistance in MRI explorations.

References

- Abdul-Rahman HS, Gdeisat MA, Burton DR, Lalor MJ, Lilley F, Moore CJ (2007) Fast and robust three-dimensional best path phase unwrapping algorithm. *Appl Opt* 46:6623–6635
- Argiles JM, Busquets S, Felipe A, Lopez-Soriano FJ (2006) Muscle wasting in cancer and ageing: cachexia versus sarcopenia. *Adv Gerontol* 18:39–54
- Azzabou N, Loureiro de Sousa P, Caldas E, Carlier PG (2015) Validation of a generic approach to muscle water T2 determination at 3T in fat-infiltrated skeletal muscle. *J Magn Reson Imaging* 41:645–653
- Cotofana S, Hudelmaier M, Wirth W, Himmer M, Ring-Dimitriou S, Sanger AM, Eckstein F (2010) Correlation between single-slice muscle anatomical cross-sectional area and muscle volume in thigh extensors, flexors and adductors of perimenopausal women. *Eur J Appl Physiol* 110:91–97
- D'Antona G, Lanfranconi F, Pellegrino MA, Brocca L, Adami R, Rossi R, Moro G, Miotti D, Canepari M, Bottinelli R (2006) Skeletal muscle hypertrophy and structure and function of skeletal muscle fibres in male body builders. *J Physiol Lond* 570:611–627
- Delmonico MJ, Harris TB, Visser M, Park SW, Conroy MB, Velasquez-Mieyer P, Boudreau R, Manini TM, Nevitt M, Newman AB, Goodpaster BH, A Health Body (2009) Longitudinal study of muscle strength, quality, and adipose tissue infiltration. *Am J Clin Nutr* 90:1579–1585
- Forsberg AM, Nilsson E, Werneman J, Bergstrom J, Hultman E (1991) Muscle composition in relation to age and sex. *Clin Sci (Lond)* 81:249–256
- Frantzell A, Ingelmark BE (1951) Occurrence and distribution of fat in human muscles at various age levels; a morphologic and roentgenologic investigation. *Acta Soc Med Ups* 56:59–87
- Glover GH, Schneider E (1991) Three-point Dixon technique for true water/fat decomposition with B0 inhomogeneity correction. *Magn Reson Med* 18:371–383
- Hasson CJ, Kent-Braun JA, Caldwell GE (2011) Contractile and non-contractile tissue volume and distribution in ankle muscles of young and older adults. *J Biomech* 44:2299–2306
- Hernando D, Haldar JP, Sutton BP, Ma J, Kellman P, Liang ZP (2008) Joint estimation of water/fat images and field inhomogeneity map. *Magn Reson Med* 59:571–580
- Hernando D, Kellman P, Haldar JP, Liang ZP (2010) Robust water/fat separation in the presence of large field inhomogeneities using a graph cut algorithm. *Magn Reson Med* 63:79–90
- Hines CD, Yu H, Shimakawa A, McKenzie CA, Brittain JH, Reeder SB (2009) T1 independent, T2* corrected MRI with accurate spectral modeling for quantification of fat: validation in a fat-water-SPIO phantom. *J Magn Reson Imaging* 30:1215–1222
- Karampinos DC, Baum T, Nardo L, Alizai H, Yu H, Carballido-Gamio J, Yap SP, Shimakawa A, Link TM, Majumdar S (2012) Characterization of the regional distribution of skeletal muscle adipose tissue in type 2 diabetes using chemical shift-based water/fat separation. *J Magn Reson Imaging* 35:899–907
- Kawakami Y, Muraoka Y, Kubo K, Suzuki Y, Fukunaga T (2000) Changes in muscle size and architecture following 20 days of bed rest. *J Gravity Physiol* 7:53–59
- Kent-Braun JA, Ng AV, Young K (2000) Skeletal muscle contractile and noncontractile components in young and older women and men. *J Appl Physiol* 88:662–668
- Kouzaki M, Masani K, Akima H, Shirasawa H, Fukuoka H, Kanehisa H, Fukunaga T (2007) Effects of 20-day bed rest

- with and without strength training on postural sway during quiet standing. *Acta Physiol (Oxf)* 189:279–292
- Leskinen T, Sipilä S, Alen M, Cheng S, Pietiläinen KH, Usenius JP, Suominen H, Kovanen V, Kainulainen H, Kaprio J, Kujala UM (2009) Leisure-time physical activity and high-risk fat: a longitudinal population-based twin study. *Int J Obes* 33:1211–1218
- Macaluso A, Nimmo MA, Foster JE, Cockburn M, McMillan NC, De Vito G (2002) Contractile muscle volume and agonist-antagonist coactivation account for differences in torque between young and older women. *Muscle Nerve* 25:858–863
- Maden-Wilkinson TM, Degens H, Jones DA, McPhee JS (2013) Comparison of MRI and DXA to measure muscle size and age-related atrophy in thigh muscles. *J Musculoskelet Neuronal Interact* 13:320–328
- McPhee JS, Hogrel JY, Maier AB, Seppet E, Seynnes OR, Sipilä S, Bottinelli R, Barnouin Y, Bijlsma AY, Gapeyeva H, Maden-Wilkinson TM, Meskers CG, Pääsuke M, Sillanpää E, Stenroth L, Butler-Browne G, Narici MV, Jones DA (2013) Physiological and functional evaluation of healthy young and older men and women: design of the European MyoAge study. *Biogerontology* 14:325–337
- Morse CI, Thom JM, Birch KM, Narici MV (2005a) Changes in triceps surae muscle architecture with sarcopenia. *Acta Physiol Scand* 183:291–298
- Morse CI, Thom JM, Mian OS, Muirhead A, Birch KM, Narici MV (2005b) Muscle strength, volume and activation following 12-month resistance training in 70-year-old males. *Eur J Appl Physiol* 95:197–204
- Morse CI, Degens H, Jones DA (2007) The validity of estimating quadriceps volume from single MRI cross-sections in young men. *Eur J Appl Physiol* 100:267–274
- Narici MV, Maganaris CN, Reeves ND, Capodaglio P (2003) Effect of aging on human muscle architecture. *J Appl Physiol* 95:2229–2234
- Nilwik R, Snijders T, Leenders M, Groen BB, van Kranenburg J, Verdijk LB, van Loon LJ (2013) The decline in skeletal muscle mass with aging is mainly attributed to a reduction in type II muscle fiber size. *Exp Gerontol* 48:492–498
- Ogawa M, Yasuda T, Abe T (2012) Component characteristics of thigh muscle volume in young and older healthy men. *Clin Physiol Funct Imaging* 32:89–93
- Overend TJ, Cunningham DA, Paterson DH, Lefcoe MS (1992) Thigh composition in young and elderly men determined by computed tomography. *Clin Physiol* 12:629–640
- Piepoli MF, Kaczmarek A, Francis DP, Davies LC, Rauchhaus M, Jankowska EA, Anker SD, Capucci A, Banasiak W, Ponikowski P (2006) Reduced peripheral skeletal muscle mass and abnormal reflex physiology in chronic heart failure. *Circulation* 114:126–134
- Reeder SB, Pineda AR, Wen Z, Shimakawa A, Yu H, Brittain JH, Gold GE, Beaulieu CH, Pelc NJ (2005) Iterative decomposition of water and fat with echo asymmetry and least-squares estimation (IDEAL): application with fast spin-echo imaging. *Magn Reson Med* 54:636–644
- Reeder SB, Robson PM, Yu H, Shimakawa A, Hines CD, McKenzie CA, Brittain JH (2009) Quantification of hepatic steatosis with MRI: the effects of accurate fat spectral modeling. *J Magn Reson Imaging* 29:1332–1339
- Roubenoff R (2000) Acquired immunodeficiency syndrome wasting, functional performance, and quality of life. *Am J Manag Care* 6:1003–1016
- Sharma SD, Hu HH, Nayak KS (2012) Accelerated water-fat imaging using restricted subspace field map estimation and compressed sensing. *Magn Reson Med* 67:650–659
- Stein TP, Wade CE (2005) Metabolic consequences of muscle disuse atrophy. *J Nutr* 135:1824S–1828S
- Trappe TA, Lindquist DM, Carrithers JA (2001) Muscle-specific atrophy of the quadriceps femoris with aging. *J Appl Physiol* 90:2070–2074
- Verdijk LB, Koopman R, Schaart G, Meijer K, Savelberg HH, van Loon LJ (2007) Satellite cell content is specifically reduced in type II skeletal muscle fibers in the elderly. *Am J Physiol Endocrinol Metab* 292:E151–E157
- Vermeeren MAP, Creutzberg EC, Schols A, Postma DS, Pieters WR, Roldaan AC, Wouters EFM, Grp CS (2006) Prevalence of nutritional depletion in a large out-patient population of patients with COPD. *Respir Med* 100:1349–1355
- Visser M, Kritchevsky SB, Goodpaster BH, Newman AB, Nevitt M, Stamm E, Harris TB (2002) Leg muscle mass and composition in relation to lower extremity performance in men and women aged 70 to 79: The health, aging and body composition study. *J Am Geriatr Soc* 50:897–904